The Plant Cell, Vol. 8, 463–475, March 1996 © 1996 American Society of Plant Physiologists

Leaf permease1 Gene of Maize Is Required for Chloroplast Development

Neil P. Schultes,[a,1] Thomas P. Brutnell,[a,2] Ashley Allen,[a] Steven L. Dellaporta,[a] Timothy Nelson,[a,3] and Jychian Chen [b]

[a] Department of Biology, Yale University, New Haven, Connecticut 06511
[b] Institute of Molecular Biology, Academica Sinica, Taipei 11529, Taiwan, Republic of China

Adjacent bundle sheath and mesophyll cells cooperate for carbon fixation in the leaves of C4 plants. Mutants with compromised plastid development should reveal the degree to which this cooperation is obligatory, because one can assay whether mesophyll cells with defective bundle sheath neighbors retain C4 characteristics or revert to C3 photosynthesis. The *leaf permease1-mutable1* (*lpe1-m1*) mutant of maize exhibits disrupted chloroplast ultrastructure, preferentially affecting bundle sheath choroplasts under lower light. Despite the disrupted ultrastructure, the metabolic cooperation of bundle sheath and mesophyll cells for C4 photosynthesis remains intact. To investigate this novel mutation, the *Activator* transposon-tagged allele and cDNAs corresponding to the *Lpe1* mRNA from wild-type plants were cloned. The *Lpe1* gene encodes a polypeptide with significant similarity to microbial pyrimidine and purine transport proteins. An analysis of revertant sectors generated by *Activator* excision suggests that the *Lpe1* gene product is cell autonomous and can be absent up to the last cell divisions in the leaf primordium without blocking bundle sheath chloroplast development.

INTRODUCTION

The photosynthetic leaf cells of higher plants rely on many intracellular and intercellular interactions for their differentiation and function. Nuclear, plastid, and mitochondrial gene expression are coordinated for the development and metabolism of photosynthetic cells (Mullet, 1988). Intracellular interactions in the form of metabolite transfer between cytosol and organelles maintain photosynthesis, respiration, and other metabolic processes in differentiated leaf cells (Raghavendra et al., 1994). In addition, intercellular interactions are particularly important in plants that perform C4 carbon fixation, a process dependent on the metabolic cooperation and structural differentiation of two dissimilar photosynthetic cells. Leaves of C4 plants, such as maize, display Kranz anatomy, in which veins are surrounded by an inner layer of photosynthetic bundle sheath cells and an outer layer of photosynthetic mesophyll cells. Each cell provides a unique subset of the required enzymatic activities for C4 photosynthesis, due mainly to cell-specific expression of the genes encoding C4 pathway enzymes (Laetsch, 1974; Nelson and Langdale, 1992, 1993). The differentiation and photosynthetic function of bundle sheath and mesophyll cells rely on light and on positional information that is as yet poorly understood. In the absence of light and positional context, photosynthetic cells differentiate with a "default" pattern of enzymatic activities suitable for C3 carbon fixation (reviewed in Nelson and Langdale, 1992, 1993).

A genetic approach provides the means to interrupt and dissect the intracellular and intercellular interactions that direct C4 cell development and function. Maize is well suited for mutational analysis of this pathway because the large seed endosperm supports substantial leaf development in plants with severe metabolic or developmental defects. The distinct cellular morphologies and metabolic roles of bundle sheath and mesophyll cells make it feasible to recover mutations with bundle sheath– or mesophyll-specific phenotypes. Among these should be mutations in "upstream" genes that influence cell identity and in "downstream" genes that perform cell differentiation. Mutations in both classes should affect bundle sheath and mesophyll cell interactions. Although many pigment-deficient, seedling-lethal, and leaf pattern mutations have been described in maize and other C4 plants, few mutations of these two classes have been identified. A potential member of the upstream class, *bundle sheath defective1–mutable1* (*bsd1-m1*), affects bundle sheath chloroplast development but not neighboring mesophyll cell chloroplasts (Langdale and Kidner, 1994). The C4 pattern of enzyme accumulation in *bsd1-m1* plants is disrupted early in development and before light-activated plastid maturation, suggesting that the wild-type gene has a regulatory role. Cell-specific or cell-preferential defects likely to fall in the downstream class are found among the many maize high chlorophyll fluorescence

[1] Current address: Department of Biochemistry and Genetics, Connecticut Agricultural Experiment Station, New Haven, CT 06504.
[2] Current address: Department of Plant Science, University of Oxford, Oxford, UK.
[3] To whom correspondence should be addressed.

(*hcf*) mutants. For example, the *hcf3* mutant is deficient in mesophyll cell–specific photosystem II thylakoid complexes (Metz and Miles, 1982).

Here, we characterize a mutation, *leaf permease1* (*lpe1*), that affects both bundle sheath and mesophyll chloroplasts under field conditions but preferentially affects bundle sheath chloroplasts under lower light intensity. The *lpe1-m1* allele was generated by insertional mutagenesis with the maize transposable element *Activator* (*Ac*), facilitating cloning of the disrupted gene. A cDNA corresponding to wild-type *Lpe1* mRNA encodes a hydrophobic polypeptide with significant similarity to bacterial uracil permeases and to a fungal xanthine transporter. Both the structure of the predicted protein and the phenotype of the *lpe1-m1* mutant suggest that the gene product is cell autonomous and essential for full chloroplast development. Although photosynthetic capacity is compromised, mutant bundle sheath and mesophyll cells are still linked metabolically for C4 photosynthesis.

RESULTS

lpe1-m1 Phenotype

A mutation showing a somatically unstable pale green phenotype segregated in a screen of M_2 families from individual selfed kernels enriched for *Ac* transpositions from the *P-vv* locus on chromosome 1S in maize (Dellaporta and Moreno, 1993). Plants homozygous for the *lpe1-m1* allele displayed a somatically unstable pale green phenotype. Sectors of normal dark green tissue appeared on a background of pale green mutant tissue. The dark green somatic sectors were large, presumably representing *Ac* excision events early in leaf development, as seen in Figure 1A, or were numerous and small, indicative of *Ac* excision late in leaf development, as seen in Figure 1B. Mutants grew to maturity with large revertant sectors or with numerous small revertant sectors. However, mutants with few revertant sectors only survived under greenhouse conditions, remained very small, and failed to produce functional floral organs.

The *lpe1-m1* pigment-deficient phenotype is light intensity–dependent. At low light intensity (50 $\mu E\ m^{-2}\ sec^{-1}$), the mutant seedling leaf tissue was visibly indistinguishable from that of wild-type siblings, whereas at higher light intensity (300 $\mu E\ m^{-2}\ sec^{-1}$), mutant leaf tissue was pale green and clearly discernible from wild-type tissue. Under field conditions ($\sim$2000 $\mu E\ m^{-2}\ sec^{-1}$), mutant tissue appeared pale green to yellow. The chlorophyll content of mutant leaf tissue was significantly lower than that of wild-type siblings at both 50 and 300 $\mu E\ m^{-2}\ sec^{-1}$, as shown in Table 1.

lpe1-m1 plants exhibited a cell-autonomous, defective-chloroplast phenotype most apparent in bundle sheath cells. Mutant and revertant bundle sheath cells were easily distinguished at the light microscope level of resolution due to the differences in plastid size and number. In mature, field-grown leaf blade tissue, bundle sheath cells in mutant sectors contained abnormally small chloroplasts, as shown in Figure 2, and $\sim$50% fewer chloroplasts than in revertant sectors (data not shown). In contrast to the striking difference between mutant and revertant bundle sheath chloroplasts, revertant-sector mesophyll chloroplasts stained with only slightly greater intensity than did neighboring mutant mesophyll chloroplasts. In dark green revertant sectors, chloroplasts of bundle sheath and mesophyll cells were indistinguishable from those in wild-type sibling plants. The mutation did not appear to alter overall leaf architecture, vasculature, or Kranz anatomy.

To determine whether bundle sheath cells contained a mixture of wild-type and mutant chloroplasts, $\sim$1000 bundle sheath cells were reconstructed from serial transverse sections from

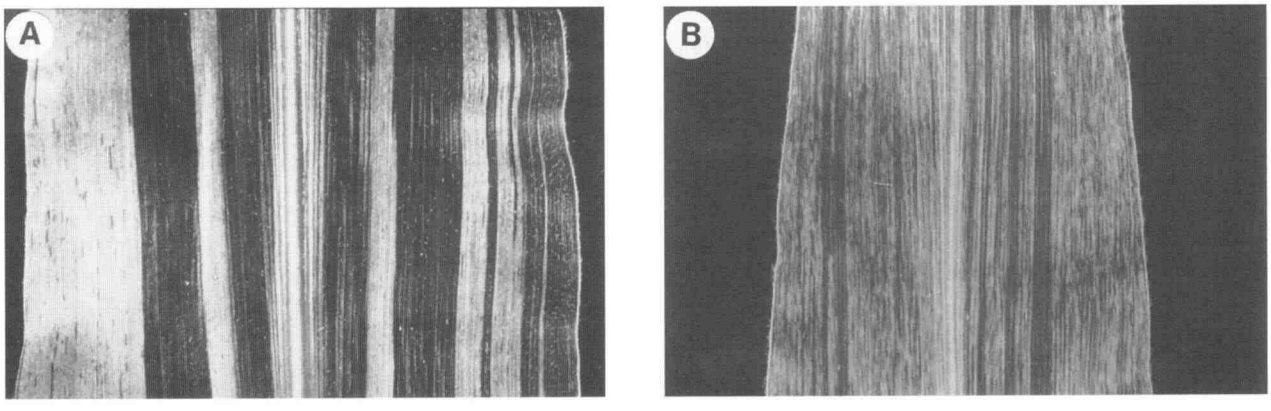

Figure 1. *lpe1-m1/lpe1-m1* Leaf Phenotype.

Field-grown adult leaves of *lpe1-m1* plants display somatic instability of dark green revertant sectors (in black) on a yellow to pale green mutant background (gray region).

(A) Revertant sectors that are large and infrequent.

(B) Revertant sectors that are small and numerous.

Table 1. Leaf Chlorophyll Concentration and Light Intensity

Light Intensity	Mutant	Wild Type	Significance[a]
50 μE m^{-2} sec^{-1}	2.74 (± 0.415) μg chlorophyll *a* and *b* per mg leaf tissue	3.28 (± 0.484) μg chlorophyll *a* and *b* per mg leaf tissue	$P < 0.015$
300 μE m^{-2} sec^{-1}	1.51 (± 0.183) μg chlorophyll *a* and *b* per mg leaf tissue	2.17 (± 0.0309) μg chlorophyll *a* and *b* per mg leaf tissue	$P < 4 \times 10^{-6}$

[a] Student's *t* test for the difference between the mutant and wild type at a given light intensity.

a mature, field-grown leaf blade containing mutant and revertant sectors (data not shown). Individual bundle sheath cells were found to contain plastids of either mutant or wild-type morphology but never a mixture of both. In addition, many single bundle sheath cell revertants were observed, representing reversion events occurring very late in leaf development. This finding suggests that the *Lpe1* gene product can act relatively late in development. The clear morphological distinction between revertant and mutant bundle sheath cells suggests that the *Lpe1* gene product acts in a cell-autonomous manner.

Plastids of Mutant Mesophyll and Bundle Sheath Cells Differ in Ultrastructural Defects

The chloroplasts of bundle sheath and mesophyll cells from mature, field-grown mutant leaf blade tissue were examined by transmission electron microscopy. Bundle sheath chloroplasts in mutant tissue were small (4.1 μm average length), contained few or no starch granules, and had on average 15 unstacked thylakoids, as represented in Figure 3A. These mutant sausage-shaped organelles had numerous plastoglobuli (carotenoid-containing bodies) at either pole and were enveloped by a swollen peripheral reticulum, which in many cases consisted of four or five layers. The peripheral reticulum is a layered membrane elaboration of unknown function often associated with chloroplasts of C4 plants (Douce et al., 1985) but normally in less abundance than observed in these mutant bundle sheath chloroplasts. Mesophyll chloroplasts in mutant tissue were of normal size and shape but lacked the extensive granal stacks characteristic of normal mesophyll chloroplasts, as seen in Figure 3B. In contrast, bundle sheath and mesophyll chloroplasts in revertant sectors appeared normal in morphology. Bundle sheath chloroplasts were large (8 mm average length), had ~20 unstacked thylakoids, were packed with numerous large starch granules, and did not have a swollen peripheral reticulum, as represented in Figure 3C. Mesophyll chloroplasts in revertant sectors appeared normal, with highly stacked grana (Figure 3C). The mitochondria in mutant bundle sheath and mesophyll cells appeared normal in size and morphology (data not shown).

The plastid phenotype appeared to be bundle sheath–specific at lower light intensity, although the alterations were less severe. We examined the chloroplasts of mutant seedlings grown at 1000 μE m^{-2} sec^{-1} illumination (half solar), a level sufficient to cause extensive photodamage in most carotenoid-deficient mutants. Figure 3D shows that mutant mesophyll cell chloroplasts grown under half-solar illumination contained stacked grana, similar in appearance to the wild type. Mutant bundle sheath chloroplasts were small, had few thylakoids, and lacked large starch granules but did not exhibit excessive peripheral reticulum or numerous plastoglobuli, as shown in Figure 3E. The swollen peripheral reticulum in bundle sheath chloroplasts and the unstacked grana of mesophyll chloroplasts in field-grown mutant tissue may have resulted from secondary damage and occurred only at high light intensity, possibly in association with the observed pigment deficiency. It is also possible that the differences observed in mutant chloroplasts grown under different light intensities (compare Figures 3A and 3B with Figures 3D and 3E) are due either to the different developmental ages of leaf tissue or to a combination of leaf age and light intensity.

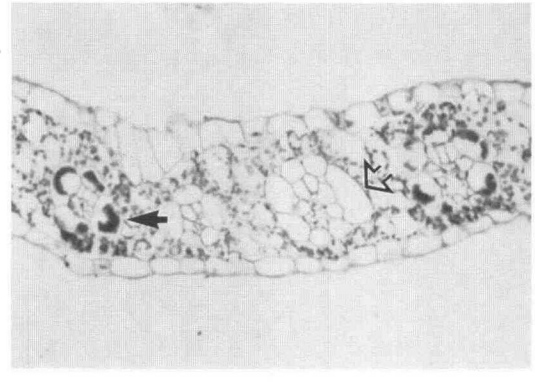

Figure 2. Histological Examination of *lpe1-m1* Leaf Tissue.

A transverse section through mature *lpe1-m1* tissue is shown. Revertant bundle sheath cells (closed arrow) contain wild-type chloroplasts. Mutant bundle sheath cells (open arrow) contain small, poorly staining chloroplasts. Mesophyll cells in revertant sectors contain chloroplasts that stain slightly more than chloroplasts in mesophyll cells of mutant sectors.

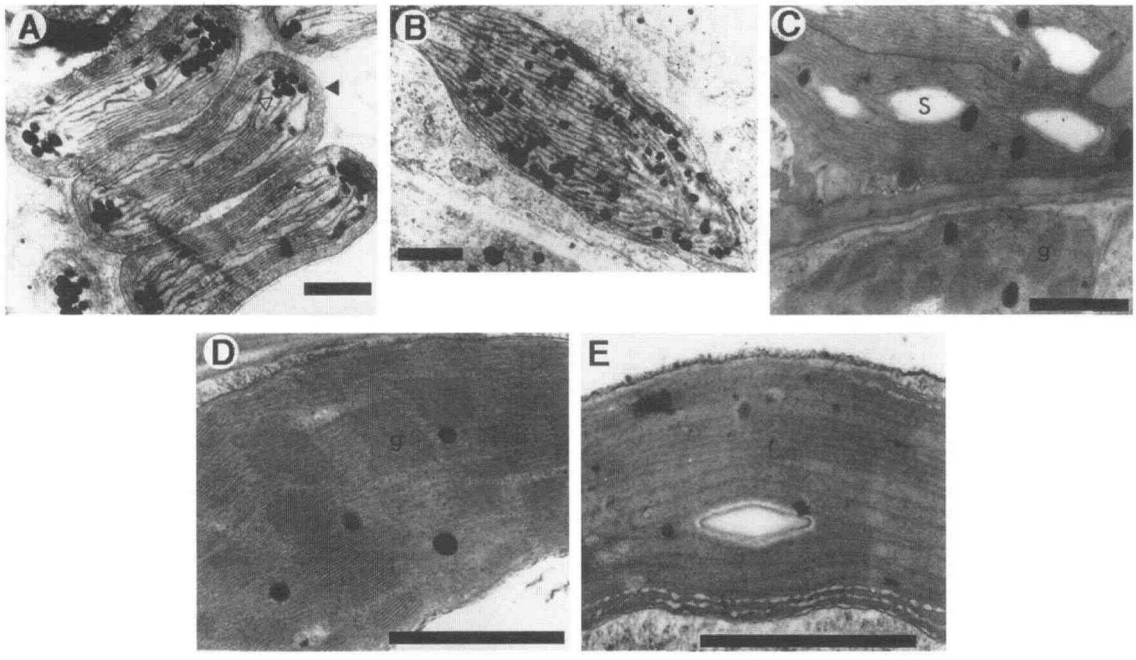

Figure 3. Chloroplast Ultrastructure.

(A) Mutant bundle sheath chloroplasts. Sections were prepared from mature, field-grown *lpe1-m1* tissue. Swollen peripheral reticulum (closed arrowhead) is present at the chloroplast border, few small starch granules are present, and plastoglobuli (open arrowhead) segregate to poles.
(B) Mutant mesophyll chloroplast. Sections were prepared from mature, field-grown *lpe1-m1* tissue. Note the lack of highly stacked grana.
(C) Revertant-bundle sheath and mesophyll chloroplasts. Sections were prepared from field-grown *lpe1-m1* revertant-sector tissue. Note the lack of swollen peripheral reticulum, the numerous thylakoids and large starch granules (S) in bundle sheath chloroplasts, and the highly stacked grana (g) in mesophyll chloroplasts.
(D) Mutant mesophyll chloroplast. The section was prepared from *lpe1-m1* mutant sector tissue of seedlings grown at 1000 μE m^{-2} sec^{-1} illumination. Note the highly stacked grana (g).
(E) Mutant bundle sheath chloroplast. The section was prepared from *lpe1-m1* mutant sector tissue of seedlings grown at 1000 μE m^{-2} sec^{-1} illumination. Note the lack of excessive peripheral reticulum yet the lack of substantial starch granules.
Bars in **(A)** to **(E)** = 1 μm.

lpe1-m1 Is Caused by *Ac* Element Insertion

Several lines of evidence indicate that an *Ac* element disrupts *Lpe1* and is responsible for the mutant phenotype. First, the mutation arose in a nondirected transposon-tagging mutagenesis in which M_1 seed were enriched for both *Ac* transposition and reinsertion elsewhere in the genome, as described by Dellaporta and Moreno (1993). Second, the somatic instability of the *lpe1-m1* mutation (Figures 1A and 1B) is characteristic of transposon-induced leaf phenotype mutations, such as *pale green14*, *bundle sheath defective1*, and *yellow1-mum* (Peterson, 1960; Buckner et al., 1990; Langdale and Kidner, 1994), which display randomly placed revertant sectors across the leaf. Third, the frequency and amount of *Lpe1* revertant sectors depended on *Ac* dosage. As the copy number of *Ac* elements in the genome increased, the frequency of revertant sectors decreased (data not shown). Fourth, *Ac* was genetically linked to the mutation. Figure 4B shows that a novel *Ac*-containing genomic fragment, lpe-m, was found in the DNA of all mutants (lanes 1 to 6), and in that of a subset of phenotypically wild-type siblings (presumed heterozygotes) (lanes 7, 9, 11, and 12), as expected for a recessive mutation. Fifth, *Ac* excision from *Lpe1* was associated with the presence of wild-type revertant sectors in the mutants. Mutant tissue should contain two *lpe1-m1* chromosomes, whereas revertant tissue will be typically heterozygous for the *lpe1-m1* and *Lpe1*-revertant chromosomes (Figure 4A).

DNA gel blot analysis of genomic PstI-digested DNA probed with an *Lpe1*-specific probe showed that mutant tissue contained predominantly the *Ac*-containing fragment (Figure 4C, lanes 1, 5, and 7), whereas the revertant tissue had both *Ac*-containing and *Ac*-excision fragments (lanes 2 to 4, 6, and 8). The difference between the mutant fragment and the revertant fragment was approximately the length of the *Ac* element (4.5 kb). The proportion of the revertant *Lpe1* fragment within phenotypically mutant tissue (e.g., Figure 4C, lanes 1 and 7) corresponded approximately to the amount of small, dark green revertant sectors observed in the mutant tissue (compare

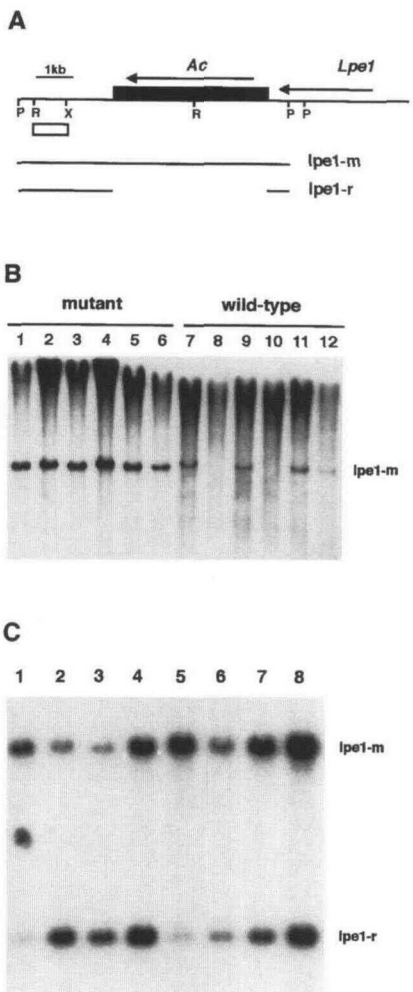

Figure 4. The *Lpe1* Gene Is Tagged by an *Ac* Element.

(A) *Lpe1-m1* DNA representation. The solid box represents the *Ac* element inserted into the *Lpe1* gene (solid line). Arrows represent the direction of transcription for the *Ac* element and *Lpe1* gene, based on sequence analysis. The open box denotes the *Lpe1*-specific 3′ genomic fragment used as a probe for DNA and RNA gel blot analyses. lpe1-m indicates the 7.9-kb PstI restriction endonuclease fragment of the *Ac*-disrupted *Lpe1* gene. lpe1-r indicates the 3.1-kb PstI restriction endonuclease fragment of the revertant *Lpe1* gene without the *Ac* insertion (see **[B]** and **[C]**). P, PstI; R, EcoRI; X, XhoI.

(B) Segregation analysis. A novel *Ac* restriction endonuclease fragment segregated among *lpe1-m1*–bearing F_2 seedlings. Lanes 1 to 6 contain genomic DNA isolated from *lpe1-m1* seedlings digested with the PstI restriction endonuclease. Lanes 7 to 12 contain PstI-digested DNA from phenotypically wild-type siblings. The blot was probed with internal *Ac* sequences (see Methods).

(C) Revertant-sector analysis. DNA from mutant (lanes 1, 5, and 7) and revertant sectors (lanes 2 to 4, 6, and 8) in three mutants (1086-1,1194-7, and122-14) was cleaved with the PstI restriction endonuclease and probed with the *Lpe1*-specific 3′ genomic fragment (shown in **[A]**). lpe1-m and lpe1-r refer to the *Ac*-containing and *Ac* excision fragments described in **(A)**.

Figures 1A and 1B). Pale green tissue was not expected to be entirely isogenic due to the combination of late *Ac* excision events resulting in small sectors and phenotypically invisible revertant sectors of any size in the epidermis. Sixth, sequence comparison of the *Ac*-tagged *Lpe1* gene and the corresponding cDNA revealed that the novel *Ac* element had inserted into the middle of an intron, as indicated in Figure 5A. Excision of the *Ac* element from *Lpe1* frequently restored the function of the gene, as demonstrated for an *Ac* insertion at the *P* locus (Brink and Nilan, 1952).

Lpe1 Locus Encodes a Novel Protein with Similarity to Pyrimidine and Purine Transport Proteins

Several *Lpe1*-hybridizing clones were isolated from a maize seedling green leaf cDNA library. The DNA sequence of the longest clone is shown in Figure 5A. The indicated ATG codon most likely serves as a translational start because it is preceded by three stop codons in each of three reading frames and initiates a 1464-bp open reading frame followed by a 421-bp 3′ untranslated region. The *Lpe1* gene lacks two features commonly found in highly expressed plant genes: the initiation ATG context does not conform to the consensus sequences derived from highly expressed plant genes (Joshi, 1987), and the proposed 5′ untranslated region is GC rich (68%). Consistent with this finding, we showed that the gene encodes a rare mRNA found in leaves and roots (see below).

The protein predicted by the *Lpe1* cDNA consists of 487 amino acids with a predicted molecular mass of 53,228 D. Several features suggest that the Lpe1 protein is an integral membrane protein. Figure 5B shows that the predicted protein is extremely hydrophobic, consists of 47.2% hydrophobic amino acids, and displays only a small central hydrophilic region (from approximately amino acids 216 to 266). Many membrane-associated regions were predicted in this polypeptide sequence. Protein structure algorithms predicted either 10 membrane-spanning segments (Klein et al., 1985), 12 membrane-associated helices (seven transmembrane, three surface, and two globular) (Eisenberg et al., 1984), or five transmembrane helices (Rao and Argos, 1986). As expected for integral membrane proteins (Klein et al., 1985), DNA binding motifs or coiled-coil regions were not found. Potential mitochondrial and chloroplast transit peptide motifs and cleavage sites were not apparent in the Lpe1 protein sequence (von Heijne et al., 1989; Gavel and von Heijne, 1990a, 1990b).

The Lpe1 protein showed a limited but significant amino acid sequence similarity to several membrane-associated permease proteins. Statistically significant similarity was found to uracil permeases from *Bacillus caldolyticus*, *B. subtilis*, and *Escherichia coli*, to hypothetical proteins from *B. subtilus* and *Clostridium perfringens*, and to a uric acid–xanthine permease from the filamentous fungus *Aspergillus nidulans* (Figure 5B). The region of greatest similarity, between amino acids 345 and 432 (Figure 5C), included a membrane-spanning segment predicted by all three aforementioned algorithms. Several

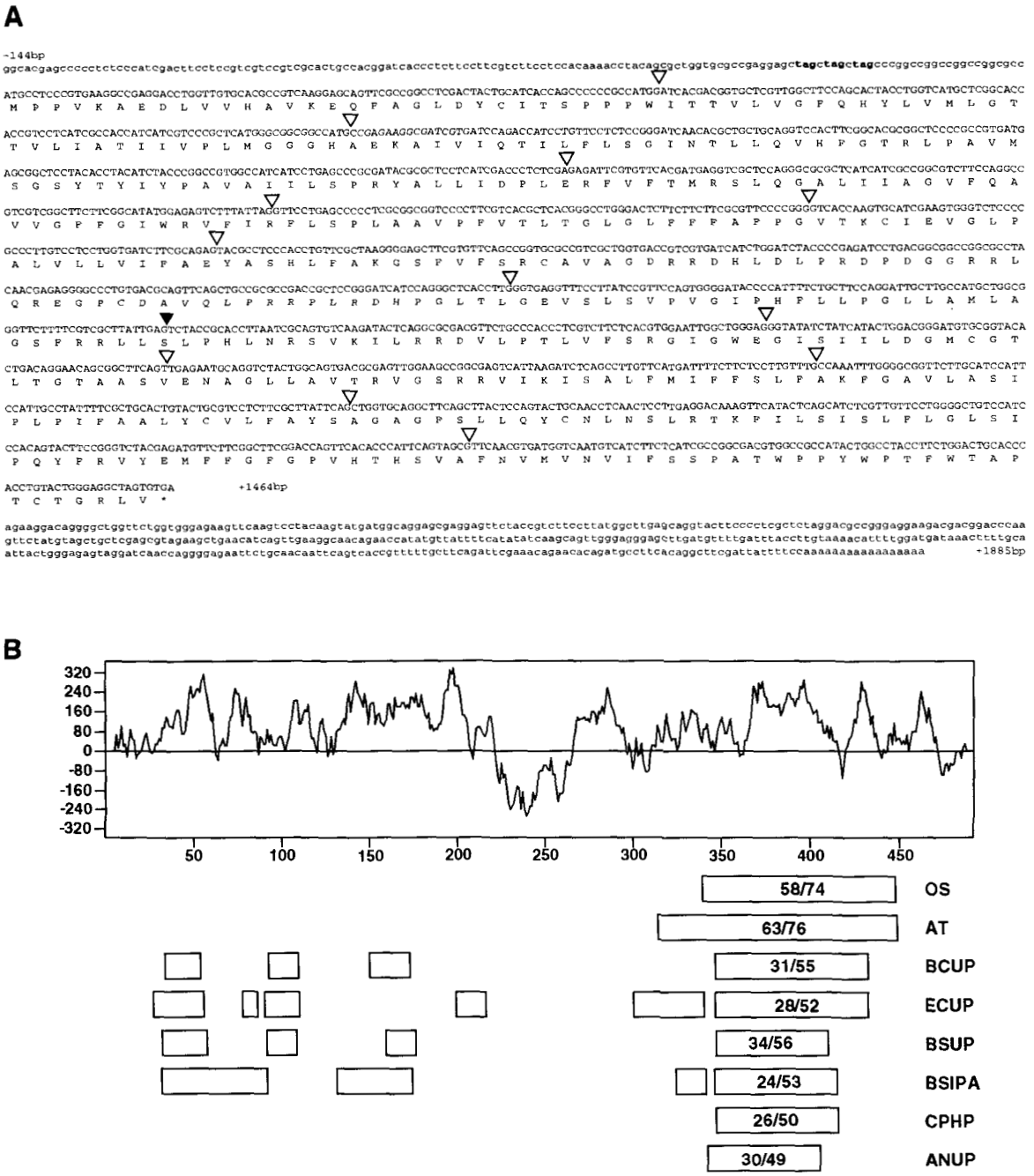

Figure 5. Sequence Analysis.

smaller patches of similarity were found in colinear fashion between the Lpe1 protein and the *Bacillus* and *Escherichia* uracil permeases (Figure 5B), suggesting a similar domain organization. The Lpe1 protein was highly similar to proteins predicted by rice and Arabidopsis-expressed sequence tag clones (Figures 5B and 5C).

Lpe1 mRNA Accumulation

Figure 6 shows that an *Lpe1* gene probe detected low levels of a 1.9-kb transcript in roots and in dark-grown leaves but not in green leaves from wild-type plants. The steady state level was approximately six- to eightfold lower in dark-grown leaves than in roots, based on digitized image analysis of autoradiographs. The *Lpe1* transcript was more abundant in the root and shoot of young seedlings germinated in the dark for 3 days than in the expanded portions of 10-day-old etiolated seedling leaves (data not shown). The *Lpe1* transcript is present in dark-grown leaves (Figure 6A, lane 2) but is less abundant after 24 hr of illumination (Figure 6A, lane 3). The transcript remains undetectable in light-grown leaves 12, 24, or 48 hr after a shift to darkness (Figure 6A, lane 5, for the 24-hr time point; 12- and 48-hr data not shown).

Mapping and Allelism Tests for *Lpe1*

The *lpe1* locus was mapped to chromosome 1L by using both recombinant inbred lines and B-A translocation lines. *lpe1-m1* heterozygotes were crossed to B-A translocation lines with break points on chromosome 1S or 1L. Of the F_1 progeny from such crosses, 6% (8/133) were pale green and mitotically unstable. The mutable pale green plants had the runty architecture and slender leaves characteristic of chromosome 1 hypoploid plants, suggesting that the recessive allele had been "uncovered" by the loss of the wild-type allele on 1L. The *Lpe1* locus was more precisely located to chromosome 1L (map position 88) by DNA gel blot analysis of recombinant inbred families (Burr et al., 1988). The *Lpe1* locus was 12.5 centimorgans (cM) from marker *bnl*17.06, 18.7 cM from the *Bronze2* locus, and 23.3 cM from marker *bnl*8.10.

Complementation tests were performed between *lpe1-m1* and several other mutations on chromosome 1. F_1 seedling analysis revealed that the *lpe1-m1* mutation was not allelic to *pale green15* (chromosome 1S), or to *pale green16*, *green stripe1*, *white luteus5*, or *lemon white1* (chromosome 1L), or to the adjacent *fine stripe1* (1L-86) to a significance of $P < 0.01$. In addition, genetic and molecular tests showed that *lpe1* is not allelic to *bsd1* (J. Langdale, personal communication). Because the *lpe1-m1* mutants did not exhibit high chlorophyll fluorescence when dark adapted and irradiated with UV illumination, no complementation tests were performed with the many *hcf* mutations that map to chromosome 1L.

Bundle Sheath and Mesophyll Cells Continue to Cooperate for C4 Metabolism in *lpe1-m1* Tissue

The apparent disruption of bundle sheath chloroplasts in *lpe1-m1* homozygotes provided an opportunity to test the metabolic cooperation of bundle sheath and mesophyll cells. We reasoned that development of photosynthetic metabolism in mesophyll cells may compensate for loss of its bundle sheath C4 partner by reverting to C3-type carbon fixation (Langdale et al., 1988). Alternatively, mutant tissue may fail to perform photosynthesis or may perform C4 photosynthesis at a greatly reduced level. These possibilities can be distinguished by

---

Figure 5. (continued).

(A) *Lpe1* cDNA sequence. Nucleotides in boldface represent amber stop codons **(tag)** preceding the large open reading frame. Open triangles indicate the insertion point of known introns, and the solid triangle indicates the start of the intron in which the *Ac* element inserted in the *Lpe1* gene. This intron is 267 bp long, and the *Ac* element is located between 138 and 139 bp 5′ to 3′. Lowercase letters denote nucleotides in the proposed untranslated regions, whereas uppercase letters denote nucleotides in the proposed coding region. Amino acids given in the single-letter abbreviation below DNA codons denote the sequence of the proposed Lpe1 protein. The GenBank accession number is U43034.

(B) Lpe1 protein homology and hydropathy plot (Kyte and Doolittle, 1984). Numbers along the plot's bottom border indicate the amino acid position in the Lpe1 protein. Open bars below the plot represent areas of amino acid similarity between the Lpe1 protein and other plant, bacterial, and fungal proteins, as determined by BLAST analysis (Altshul et al., 1990). OS, *Oryza sativa* translation of an expressed sequence tag (DDBJ accession number D28174); AT, Arabidopsis, translation from a partial sequence from an expressed sequence tag (EMBL accession number Z25495); BCUP, ECUP, and BSUP, uracil permeases from *B. caldolyticus* (Ghim and Neuhard, 1994) (EMBL accession number X76083), *E. coli* (Andersen et al., 1995) (EMBL accession number X73586), and *B. subtilus* (Turner et al., 1994) (GenBank accession number M59757), respectively; BSIPA, *B. subtilus* hypothetical open reading frame ipa-60d (Fujita et al., 1986; Glaser et al., 1993) (EMBL accession number X73124); CPHP, *C. perfringens* hypothetical protein (Brynestad et al., 1994) (PIR accession number S33349); ANUP, *A. nidulans* uric acid–xanthine permease (Gorfinkiel et al., 1993) (EMBL accession number X71807). The numbers in the open boxes represent the percentage of amino acid identity/amino acid similarity. All P values for amino acid similarity are < 0.05.

(C) Amino acid homology alignment. Shown is an expanded pairwise BLAST alignment of Lpe1 protein amino acids 339 to 429 and similar proteins (Altshul et al., 1990). Protein sequences are labeled as given in **(B)**. (+) indicates amino acid similarity; an empty space indicates an amino acid sharing no identity or similarity with the Lpe1 protein and the compared sequence; the protein sequences are linear and have no gaps in the comparison. For the Arabidopsis sequence, several open reading frames were spliced together to overcome probable DNA sequence errors.

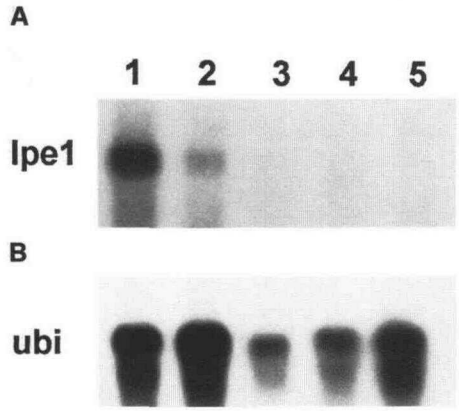

Figure 6. *Lpe1* mRNA Accumulation.

(A) *Lpe1* RNA after light shifts. RNA gel blot of poly(A)$^+$ mRNA (1 μg) isolated from seedling roots (lane 1), etiolated seedling leaves (lane 2), etiolated seedling leaves shifted to 24 hr of light (lane 3), green seedling leaves (lane 4), and green seedling leaves shifted to 24 hr of darkness (lane 5). A 1.9-kb transcript is visible in roots and etiolated leaves (lanes 1 and 2) but not in green leaves (lanes 4 and 5). The blot was probed with an *Lpe1*-specific 3′ genomic probe (see Figure 4A). **(B)** Control duplicate blot probed with maize polyubiquitin (ubi) sequences.

measuring the CO_2 compensation point of the mutant tissue. In a closed system, the CO_2 compensation point is a measure between the equlibrium of CO_2 fixation by photosynthesis and release through photorespiration. C3 plants attain an equilibrium CO_2 concentration of ~50 to 80 ppm in a closed environment, whereas C4 plants achieve levels of 1 to 10 ppm due to the low rate of photorespiration. Tissue that does not photosynthesize (e.g., roots) will generate increasing levels of CO_2 due to respiration.

CO_2 compensation points were measured for leaf tissue from both seedling and adult *lpe1-m1* mutants and sibling wild-type plants. Figures 7A and 7B show that mutant tissue achieves a low equilibrium CO_2 concentration similar to that for wild-type tissue and characteristic of functional C4 carbon fixation. However, the mutant tissue achieved equilibrium at a slower rate than did the wild-type tissue (Figures 7A and 7B), suggesting that the photosynthetic rate is reduced. To determine whether revertant leaf tissue also performs C4 photosynthesis, a leaf sample from a large revertant sector on a mature greenhouse-grown *lpe1-m1* mutant plant was compared with adjacent mutant tissue in CO_2 compensation point assays. The results in Table 2 show that both the developmentally paired mutant and the revertant tissue achieve low CO_2 compensation points (< 6 ppm). Greenhouse-grown plants were used for the measurements to reduce contributions resulting from high light intensity damage. To ensure that the compensation point of mutant tissue was not influenced by contributions from significant patches of revertant tissue, DNA derived from the same revertant and mutant tissue sectors was subjected to DNA gel blot analysis, using an *Lpe1* probe. No revertant bands were detectable in the mutant tissue (data not shown), suggesting that any contribution by revertant tissue was small.

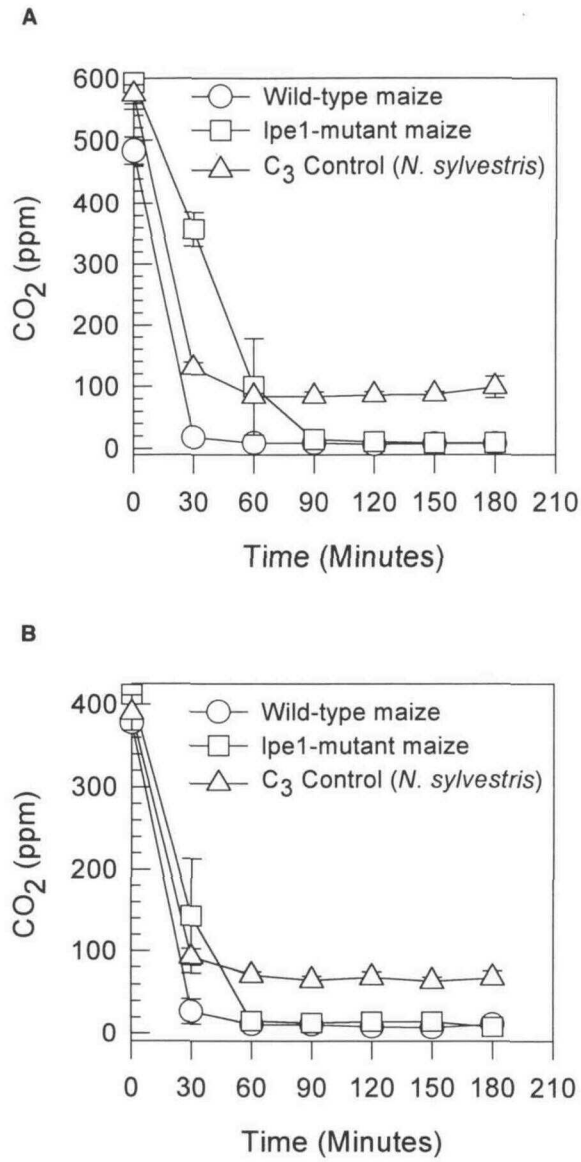

Figure 7. CO_2 Compensation Point Assays.

(A) Time course of averaged CO_2 concentration measurements for *lpe1-m1* and sibling wild-type seedling leaf tissue. *N. sylvestris* leaf tissue is a C3 control. CO_2 concentration was measured in parts per million (ppm).

(B) Time course of averaged CO_2 concentration measurements for *lpe1-m1* and sibling wild-type adult leaf tissue.

Table 2. CO_2 Compensation Point Analysis

Plant	Phenotype	CO_2 (ppm)
N. sylvestris	C3 photosynthesis control	55.2; 58
Maize	Revertant sector *Lpe1-r/lpe1-m1*	6; 3.6
Maize	Mutant sector *lpe1-m1/lpe1-m1*	1.7; 1.3

DISCUSSION

The C4 carbon fixation cycle relies on intercellular cooperation between bundle sheath and mesophyll cells and on intracellular cooperation between chloroplast and mitochondrion. Mutations that specifically or preferentially affect the function of bundle sheath or mesophyll cells represent genetic tools that can be used to investigate these interactions. We isolated one such mutation, *lpe1-m1*, which differentially affects bundle sheath and mesophyll chloroplast morphology, depending on the light intensity. The corresponding *Lpe1* gene, named for the leaf phenotype and permease homology, appears to encode an integral membrane protein that is required for normal chloroplast function.

Transposon-Induced Mutations and the Study of Gene Action

Transposable element insertions can greatly facilitate the functional analysis of target genes. First, the availability of a transposon-induced mutant allele often permits the molecular cloning of the gene by using the transposon as a molecular tag. Second, the somatic instability of many transposon-induced alleles allows the requirement for a cell-autonomous gene product to be defined in developmental time. For *lpe1-m1* plants, revertant dark green sectors reflect excision of the *Ac* element during cell divisions in the developing leaf primordium. Because most cell divisions in the leaf promordium are completed before exposure to light, the range of observed sectors delimits the period in which primordia require the Lpe1 protein. The presence of single revertant bundle sheath cells with completely restored phenotype reveals that the *Lpe1* gene product is required only late in leaf development, most likely before light-stimulated development of the bundle sheath plastids. Third, the somatic instability in mutants gives rise to adjacent mutant and revertant tissue that is isogenic (except for the allele in question) and developmentally paired. The presence of large revertant and mutant sectors in some *lpe1-m1* plants is useful for biochemical and physiological assays, such as the CO_2 compensation point analysis. The size and frequency of sectors can be controlled by genetic manipulation of transposable element dosage.

A Unique Chloroplast Phenotype in *lpe1-m1* Mutants

The plastid defects observed in *lpe1-m1* plants differ from those in previously characterized mutants in two regards. First, defects are most apparent in bundle sheath chloroplasts. The majority of maize mutants with plastid defects affect both bundle sheath and mesophyll cells (e.g., *iojap* and some carotenoid-deficient mutations; Bachmann et al., 1967; Thompson et al., 1983). Second, affected chloroplasts appear to reach a relatively advanced stage in development. In the maize mutant *bsd1*, which is bundle sheath cell specific, chloroplasts arrest early in mutant bundle sheath cells (Langdale and Kidner, 1994).

The *lpe1-m1* pale green leaf phenotype is dependent on light intensity (Table 1), as are the phenotypes of many pigment-deficient mutants. This suggests that a portion of the observed phenotype, including pigment deficiency, the hypertrophied peripheral reticulum in bundle sheath chloroplasts, and the lack of stacked grana in mesophyll chloroplasts, is the secondary consequence of photooxidation and is not the direct result of the *lpe1-m1* defect. The chlorophyll-deficient phenotype does not necessarily imply a specific biosynthetic function of the *Lpe1* gene product because a broad range of mutants fall into this phenotypic class. For example, chlorophyll biosynthetic mutants (e.g., *olive* in Antirrhinum; Hudson et al., 1993), plastid biogenesis mutants (e.g., *bsd1* in maize; Langdale and Kidner, 1994), other leaf development mutants (e.g., *pale cress* of Arabidopsis; Reiter et al., 1994), and mutations associated with mitochondrial defects (e.g., *nonchromosomal stripe2* and 6 of maize; Roussell et al., 1991; Gu et al., 1993) all display pale green leaf phenotypes. The cell-autonomous nature of revertant *lpe1-m1* bundle sheath cells suggests that Lpe1 protein function does not influence adjacent cells. Although mutant and normal cells appear to be homoplastidic, it is unclear whether the Lpe1 protein action is plastid autonomous, as is the phenotype of the *immutans* mutation of Arabidopsis (Wetzel et al., 1994).

C4 Photosynthesis and *lpe1-m1*

The cooperation of bundle sheath and mesophyll cells is essential for the function of C4 photosynthesis. A severe defect in one of the two partners should reveal the degree to which the metabolism of one is coupled to the other. For example, in the absence of a functional bundle sheath neighbor, mesophyll cells might independently perform C3 photosynthesis. Despite the apparent defects in bundle sheath cells, homozygous *lpe1-m1* tissue is capable of C4 photosynthesis, as determined by its low CO_2 compensation point (Figures 7A and 7B, and Table 2). Although we made no direct measurement of overall photosynthetic efficiency, the slower rate of attaining CO_2 equilibrium (Figures 7A and 7B) and the absence of significant starch accumulation (Figure 3A) suggest that photosynthetic efficiency is low. In addition, only mutant plants with large or numerous revertant sectors survive under field conditions or complete a full life cycle under greenhouse conditions (Figures

1A and 1B). Together, these observations suggest that bundle sheath and mesophyll metabolic cooperation are intact but that the overall photosynthetic capacity is marginal, possibly as a secondary consequence of loss of *Lpe1* function.

Regulation of *Lpe1* mRNA Accumulation

The pattern of *Lpe1* mRNA accumulation—abundant in nonleaf tissue and not detected in light-grown leaves—at first appears paradoxical for a gene product required for chloroplast development and pigment accumulation. However, *Lpe1* gene expression may be limited to early stages of development, whereas the *Lpe1* gene product plays a role that affects the plastid at that time or later. Thus, deficiencies of the *Lpe1* gene product may not become evident as a leaf phenotype until strong illumination demands its function. In addition, the pattern of regulation in leaves and the abundance in roots of the *Lpe1* mRNA are the patterns observed for other genes whose products are engaged in energy metabolism or in the intracellular exchange of metabolites between organelles (e.g., maize adenine nucleotide translocator gene; Day, 1992). Such genes might be expected to have distinct light/dark regulation in photosynthetic versus nonphotosynthetic tissues. In nonphotosynthetic tissue, such as roots and dark-grown leaves, the mitochondrion provides the sole source of energy, whereas in light-grown leaves, the chloroplast produces ATP and mitochondrial activities are reduced (Raghavendra et al., 1994). The *Lpe1* gene and its product may be involved in metabolic processes affected by illumination.

A Possible Role for *Lpe1*

We propose that the Lpe1 protein resides in the membranes of a cellular organelle in both bundle sheath and mesophyll cells, where it serves as a transporter or permease for pyrimidine or purine molecules. The predicted integral membrane nature and abundance of membrane-associated domains in the Lpe1 protein strongly suggest that this protein is localized in membranes (Figure 5B; Eisenberg et al., 1984; Klein et al., 1985; Rao and Argos, 1986). The high degree of amino acid similarity and colinearity of domains between the Lpe1 protein and bacterial and eukaryotic membrane permease proteins (Figures 5B and 5C) suggest that *Lpe1* encodes a membrane permease or transporter, possibly recognizing the purine xanthine. In some ureide-producing symbiotic N_2-fixing legumes, xanthine is a catabolic product generated in the chloroplast, then transported and converted to uric acid en route to the peroxisome (Schubert, 1986). The Lpe1 protein may be involved in a related pathway, possibly located in the chloroplast or peroxisome. Alternatively, it is also possible that the Lpe1 protein is localized in the mitochondria, because some mutations affecting mitochondrial proteins lead to chloroplast defects (Newton, 1993).

The action of the Lpe1 protein as an organellar purine or pyrimidine permease is consistent with the phenotype of *lpe1-m1* mutants. A deficiency in intracellular metabolite traffic is likely to have pleiotropic effects on dependent biochemical processes. The bundle sheath preferential nature of the phenotype may be a consequence of the greater dependence of bundle sheath cells on *Lpe1*-related metabolites. Future experiments to investigate the role of the Lpe1 protein will examine the subcellular localization of the protein in maize.

METHODS

Maize Stocks and Genetic Manipulation

The *Activator* (*Ac*) transposon mutagenesis strategy used to generate the pale green mutation has been described by Dellaporta and Moreno (1993). The original pale green stock was backcrossed into a W22 background for up to four generations. For analysis of wild-type transcripts and light effects, inbred B73 maize seedlings (Pioneer Hi-Bred, Johnston, IA) were used. Other maize stocks used in the study were obtained from the Maize Genetics Cooperation Stock Center (Urbana, IL): TB-1La (stock center No. 122A), TB-1Sb (No. 122B), *sr1/sr1* (No. 101B), *bz2/bz2* (No. X18G), *br1/br1 f1/f1* (No. 109E), *gs1/+* (No. 119C), *lw1/+* (No. 118C), *pg15/pg15* (No. 128D), *pg15/+* (No. 128D*), *pg16/+* (No. 128E), and *wlu5/+* (No. 129B).

Maize was grown under summer field conditions at the Connecticut Agricultural Experiment Station (Hamden, CT) during the summers of 1990 to 1994. For greenhouse propagation, maize was grown in Metromix 200 (Scotts-Sierra Horticultural Products Company, Maryville, OH) at ~28°C. For light-shift experiments, seedlings were grown at 28°C and either in 16-hr-light/8-hr-dark at 1000 $\mu E\ m^{-2}\ sec^{-1}$ or in complete darkness for 10 days before light-shift regimes. Sandbench growth under greenhouse conditions was used to assay seedling phenotype.

For complementation tests, pollen from plants heterozygous or homozygous for a mutation was used for selfing and for fertilization of *lpe1-m1* heterozygote ears. *Lpe1* recipient plants were confirmed as heterozygotes through DNA blot analysis or by selfing the second ear and scoring the F_1 generation for the unstable pale green phenotype in sandbench plantings.

For crosses with B-A translocation stocks affecting chromosome 1 arms, pollen from B-A plants (scored by their semiviable pollen) was used to fertilize heterozygous *lpe1-m1* plants. Pollen from B-A plants was also crossed to chromosome 1S or 1L tester stocks (*sr1/sr1* or *bz2/bz2*, respectively) to verify that a translocation was present in the donated pollen (Beckett, 1978). The phenotypes of progeny were scored in sandbenches. DNA gel blot analysis, using an *Ac*-specific probe, confirmed that the F_1 hypodiploids were hybrid plants between the B-A and *lpe1-m1* heterozygote parents and were not the result of pollen contamination from the *lpe1-m1* heterozygote.

Chlorophyll Determination

Seed from a cross of *lpe1-m1/lpe1-m1* × *Lpe1/lpe1-m1* were grown for 10 days at 50 or 300 $\mu E\ m^{-2}\ sec^{-1}$ irradiance at room temperature. All plants were verified to be *lpe1-m1* mutants or heterozygotes by DNA gel blot hybridization. Seven *lpe1-m1* seedlings and 10 heterozygote

siblings were analyzed at 50 μE m^{-2} sec^{-1}. Nine *lpe1-m1* seedlings and nine heterozygote siblings were analyzed at 300 μE m^{-2} sec^{-1}. Two 5-mm in diameter leaf discs were isolated from the third leaf midway between the leaf tip and ligule from each plant. Total chlorophyll content was estimated spectrophometrically in extracts, according to standard techniques (Coombs et al., 1985).

Histology and Electron Microscopy

For light microscopy, mature, field-grown leaf tissue was harvested, fixed, and embedded in Paraplast+ (Oxford Labware, St. Louis, MO), as described by Langdale et al. (1987). Eight-micron serial leaf cross-sections were stained with safranin-fast green by standard methods (Berlyn and Miksche, 1976) and photographed on T-MAX 100 or Ektachrome 160 film with an Axiophot microscope system (Zeiss, Oberkochen, Germany). For transmission electron microscopy analysis, field-grown 60- to 80-day post-planting, preflowering *lpe1-m1* mutant leaf tissue was harvested from the fifth to seventh leaf blade, midway between the ligule and tip. The samples were harvested on a sunny day at approximately noon, allowing time for photosynthesis and starch accumulation to occur. Tissue from leaves of plants from growth rooms was harvested from the third leaf, also midway between the ligule and tip. Samples were fixed in a solution consisting of 4% paraformaldehyde, 4% glutaraldehyde, 0.05 M phosphate buffer, pH 7.5, 0.1 M sucrose at room temperature for 2 hr, and then postfixed in 2% OsO_4 for 2 hr at room temperature and embedded in Spurr's resin. Thin sections were stained with uranyl acetate and lead citrate and viewed on a Diaplan EM-10A transmission electron microscope (Zeiss).

DNA Gel Blot Analysis

Maize genomic DNA was prepared as described by Chen and Dellaporta (1993) and Dellaporta (1993). Restriction endonuclease–digested DNA was fractionated on agarose gels (Ausubel et al. 1989) and transferred under alkaline conditions to a charged nylon membrane (Zetaprobe GT; Bio-Rad, Richmond, CA), as described by the manufacturer. Hybridization conditions were as described by Ausubel et al. (1989). Probes for DNA and RNA gel blot analyses were labeled with ^{32}P-dCTP by random priming (Feinberg and Vogelstein, 1984). These included an internal 1.6-kb HindIII fragment of *Ach*1.6 and a 1.1-kb EcoRI-BglII genomic fragment containing 3′ sequences from the *Lpe1* gene (pNS235 insert) (Figure 4A).

The novel *Ac* element and surrounding genomic DNA were cloned by standard methods as a BamHI fragment into a λ EMBL3 vector. Approximately 1 × 10^6 phage was probed with an internal *Ac* HindIII fragment (above), and a positive clone, TA69, was used for further analysis. An EcoRI fragment containing one-half of the *Ac* element with flanking 3′ genomic *Lpe1* sequences was subcloned into the pBluescript SK+ (Stratagene, San Diego, CA) and designated BMP-TA69. From this plasmid, an internal 1.1-kb EcoRI-BglII fragment was subcloned into the EcoRI and BamHI sites of plasmid pMLC28 (Levinson et al., 1984) to form pNS235.

To obtain *Lpe1* cDNAs, a cDNA library prepared from maize green seedlings (kindly provided by Alice Barkan, University of Oregon, Eugene, OR) was screened with a pNS235 insert as a probe. Approximately 10^6 plaques were screened by standard methods to yield 15 phage isolates that contained *Lpe1* sequences. Eight cDNA clones of different lengths were sequenced from their 3′ ends. The DNA sequences of all clones were identical but varied in the length of the 3′ poly(A) end. The longest cDNA isolate was completely sequenced on both DNA strands by the dideoxy chain termination method with a modified T7 polymerase (Sequenase; U.S. Biochemical, Cleveland, OH). Overlapping sequencing templates were created through subcloning, specific oligonucleotide priming, bacterial generated in vivo deletions, or bacterial transposon-facilitated priming (Sequerlap and TN1000; Gold Biotechnology, St. Louis, MO).

RNA Gel Blot Analysis

Total RNA was isolated by guanidium thiocyanate extraction (described by Nelson et al., 1984). Poly(A)$^+$-enriched RNA was prepared on Dynabead matrices, as described by the manufacturer (Dynal, Oslo, Norway). One microgram of poly(A)$^+$-enriched RNA from different samples was fractionated through formaldehyde MOPS 1.5% agarose gels (Ausubel et al., 1989) and transferred to a nylon membrane (Nytran; Schleicher & Schuell, Keene, NH). Hybridization conditions were as described for DNA gel blot analysis. For the light-shift experiment, light-grown seedling leaf samples were isolated from the blade of third leaves. For etiolated leaf samples, the entire emerging leaf blade was harvested. Root samples were harvested from light-grown seedlings germinated in Metro-mix 200. Blots were stripped and reprobed with a maize ubiquitin partial cDNA (pSKUBI) (Christensen et al., 1992) to confirm the intactness of RNA from the green leaf tissue.

Recombinant Inbred Mapping of the *Lpe1* Locus

Forty-four genomic DNA samples of recombinant inbred maize lines T232 × CM37 were cleaved with HindIII restriction endonuclease and probed with a 1.1-kb XhoI-HindIII 3′ genomic *Lpe1* fragment (contained in pNS235). Restriction fragment length polymorphisms were tabulated and used to construct a genetic map (Burr et al., 1988).

CO_2 Compensation Point Analysis

Greenhouse-grown *lpe1-m1* mutant and wild-type sibling maize seedlings (2 weeks old) and adult plants (7 weeks old; preflowering) were used for the assay (Figures 7A and 7B). A greenhouse-grown *lpe1-m1* plant displaying half-leaf sectors was used for adjacent mutant and revertant analysis at 70 days (Table 2). *Nicotiana sylvestris* (cv Speget Comes) grown under 18 hr of light at 28°C and 6 hr of darkness at 20°C was used as a C3 plant control (Figures 7A and 7B, and Table 2). For the data in Figures 7A and 7B, eight 0.5-mm leaf discs from the second and third seedling leaves or midway down the seventh and eighth blade in adult plants were harvested from each plant. Each measurement is the average of three separate plant samples. For the mutant and revertant tissue analysis, two 1.6-cm leaf discs were harvested from adjacent mutant and revertant tissue from the seventh leaf midway between the ligule and leaf tip and analyzed separately. In all assays, the leaf tissue was placed on wet Whatman No. 3MM chromatography paper and enclosed in 50-mL syringes. Five-milliliter samples were withdrawn and analyzed in an infrared analyzer (model 865; Beckman, Palo Alto, CA) over a period of 3 hr to ensure that the CO_2 concentration had reached equilibrium. Assay conditions for the seedling tissue were 26°C under 150 μE m^{-2} sec^{-1} irradiance, 25°C under 75 μE m^{-2} sec^{-1} irradiance for the adult analysis, and 27°C under 84 μE m^{-2} sec^{-1} irradiance for the revertant tissue analysis.

Computer Analysis

DNA sequence and protein sequence analyses were performed using GeneWorks 2.0 and PC Gene (Intelligenetics, Mountain View, CA). Sequence homology searches were performed on BLAST programs through National Center for Biotechnology Information (Bethesda, MD) (Altshul et al., 1990).

ACKNOWLEDGMENTS

We thank Richard Peterson (Connecticut Agricultural Experiment Station, New Haven, CT) for assistance with the CO_2 compensation point analysis, Alice Barkan (University of Oregon, Eugene, OR) for providing a maize seedling cDNA library, and Maria Moreno (Yale University, New Haven, CT) for assistance in screening the cDNA library. We thank Jane Langdale (University of Oxford, UK) for performing allelism and DNA hybridization tests between *bsd1* and *lpe1-m1*, Julia Paxson for assistance with RNA analysis, Barry Piekos for assistance with photomicrography and transmission electron microscopy, Ben Burr (Brookhaven National Laboratories, Upton, NY) for providing recombinant inbred maize lines, and Peter Quail (U.S. Department of Agriculture Plant Gene Expression Center, Albany, CA) for supplying the maize ubiquitin cDNA plasmid pSKUBI. We thank Vivian Irish (Yale University) and Neil McHale (Connecticut Agricultural Experiment Station) for helpful comments on the manuscript. This work was supported by National Institutes of Health grants No. R01-GM33984 to T.N. and No. R01-GM38148 to S.L.D.

Received September 19, 1995; accepted January 4, 1996.

REFERENCES

Altshul, S.F., Gish, W., Miller, W., Myers, E.W., and Lipman, D.J. (1990). Basic local alignment search tool. J. Mol. Biol. **215,** 403–410.

Andersen, P.S., Frees, D., Fast, R., and Mygind, B. (1995). Uracil uptake in *Escherichia coli* K-12: Isolation of *uraA* mutants and cloning of the gene. J. Bacteriol. **1770,** 2008–2013.

Ausubel, F.M., Brent, R., Kingston, R.E., Moore, D.D., Siedman, J.G., Smith, J.A., and Struhl, K., eds (1989). Short Protocols in Molecular Biology. (New York: John Wiley and Son).

Bachmann, M.D., Robertson, D.S., Bowen, C.C., and Anderson, I.C. (1967). Chloroplast development in pigment-deficient mutants of maize. J. Ultrastruct. Res. **21,** 41–60.

Beckett, J.B. (1978). B-A translocations in maize. J. Hered. **69,** 27–36.

Berlyn, G.P., and Miksche, J.P. (1976). Botanical Microtechnique and Cytochemistry. (Ames, IA: Iowa State University Press).

Brink, R.A., and Nilan, R.A. (1952). The relationship between light variegated and medium variegated pericarp in maize. Genetics **37,** 519–544.

Brynestad, S., Iwanejko, L.A., Stewart, G.S.B.A., and Granum, P. E. (1994). A complex array of Hpr consensus DNA recognition sequences proximal to the enterotoxin gene in *Clostridium perfringens* type A. Microbiology **140,** 97–104.

Buckner, B., Kelson, T.L., and Robertson, D.S. (1990). Cloning of the *y1* locus of maize, a gene involved in the biosynthesis of carotenoids. Plant Cell **2,** 867–876.

Burr, B., Burr, F.A., Thompson, K.H., Albertson, M.C., and Stuber, C.W. (1988). Gene mapping with recombinant inbreds in maize. Genetics **118,** 519–526.

Chen, J., and Dellaporta, S.L. (1993). Urea-based plant DNA miniprep. In The Maize Handbook, M. Freeling and V. Walbot, eds (New York: Springer-Verlag), pp. 526–527.

Christensen, A.H., Sharrock, R.A., and Quail, P.H. (1992) Maize polyubiquitin genes: Structure, thermal perturbation of expression and transcript splicing and promoter activity following transfer to protoplasts by electroporation. Plant Mol. Biol. **18,** 675–689.

Coombs, J., Hind, G., Leegood, R.C., Tieszen, L.L., and Vonshak, A. (1985). Analytical techniques. In Techniques in Bioproductivity and Photosynthesis, J. Coombs, D.O. Hall, S.P. Long, and J.M.O. Scurluck, eds (New York: Pergamon Press), pp. 219–228.

Day, C. (1992). The Mitochondrial Adenine Nucleotide Translocator of *Zea mays* L. Gene Structure and Expression. PhD Dissertation (Edinburgh, Scotland: University of Edinburgh).

Dellaporta, S.L. (1993). Plant DNA miniprep and microprep: Version 2.1–2.3. In The Maize Handbook, M. Freeling and V. Walbot, eds (New York: Springer-Verlag), pp. 522–525.

Dellaporta, S.L., and Moreno, M.A. (1993). Gene tagging with *Ac/Ds* elements in maize. In The Maize Handbook, M. Freeling and V. Walbot, eds (New York: Springer-Verlag), pp. 219–233.

Douce, R., Block, M.A., Dorne, A.-J., and Joyard, J. (1985). The plastid envelope membranes: Their structure, composition, and role in chloroplast biogenesis. Subcell. Biochem. **10,** 1–86.

Eisenberg, D., Schwarz, E., Komaromy, M., and Wall, R. (1984). Analysis of membrane and surface protein sequences with the hydrophobic moment plot. J. Mol. Biol. **179,** 125–142.

Feinberg, A.P., and Vogelstein, B. (1984). A technique for radiolabeling DNA restriction endonuclease fragments to high specific activity. Anal. Biochem. **137,** 266–267.

Fujita, Y., Fujita, T., Miwa, Y., Nihashi, J., and Aratani, Y. (1986). Organization and transcription of the gluconate operon, *gnt*, of *Bacillus subtilis*. J. Biol. Chem. **261,** 13744–13753.

Gavel, Y., and von Heijne, G. (1990a). A conserved cleavage site motif in chloroplast transit peptides. FEBS Lett. **261,** 455–458.

Gavel, Y., and von Heijne, G. (1990b). Cleavage-site motifs in mitochondrial targeting peptides. Protein Eng. **4,** 33–38.

Ghim, S.-Y., and Neuhard, J. (1994). The pyrimidine biosynthesis operon of the thermophile *Bacillus caldolyticus* includes genes for uracil phosphoribosyltransferase and uracil permease. J. Bacteriol. **176,** 3698–3707.

Glaser, P., Kunst, F., Arnaud, M., Coudart, M.P., Gonzales, W., Hullo, M.F., Ionescu, M., Lubochinsky, B., Marcelino, L., Moszer, I., Presecan, E., Santana, M., Schneider, E., Schweizer, J., Vertes, A., Rapoport, G., and Danchin, A. (1993). *Bacillus subtilis* genome project: Cloning and sequencing of the 97 kb region from 325° to 333°. Mol. Microbiol. **10,** 371–384.

Gorfinkiel, L., Diallinas, G., and Scazzocchio, C. (1993). Sequence and regulation of the *uapA* gene encoding a uric acid–xanthine permease in the fungus *Aspergillus nidulans*. J. Biol. Chem. **268,** 23376–23381.

Gu, J., Miles, D., and Newton, K.J. (1993). Analysis of leaf sectors in the *NCS6* mitochondrial mutant of maize. Plant Cell **5,** 963–971.

Hudson, A., Carpenter, R., Doyle, S., and Coen, E.S. (1993). *Olive*: A key gene required for chlorophyll biosynthesis in *Antirrhinum majus*. EMBO J. **12,** 3711–3719.

Joshi, C.P. (1987). An inspection of the domain between putative TATA box and translation start site in 79 plant genes. Nucleic Acids Res. **15,** 6643–6653.

Klein, P., Kanehisa, M., and DeLisi, C. (1985). The detection and classification of membrane-spanning proteins. Biochem. Biophys. Acta **815,** 468–476.

Kyte, J., and Doolittle, R.F. (1984). A simple method for displaying the hydropathic character of a protein. J. Mol. Biol. **157,** 105–132.

Laetsch, W.M. (1974). The C4 syndrome: A structural analysis. Annu. Rev. Plant Physiol. **25,** 27–52.

Langdale, J., and Kidner, C.A. (1994). *bundle sheath defective*, a mutation that disrupts cellular differentiation in maize leaves. Development **120,** 673–681.

Langdale, J.A., Metzler, M.C., and Nelson, T. (1987). The *argentia* mutation delays normal development of photosynthetic cell-types in *Zea mays*. Dev. Biol. **122,** 243–255.

Langdale, J.A., Zelitch, I., Miller, E., and Nelson, T. (1988). Cell position and light influence C4 versus C3 patterns of photosynthetic gene expression in maize. EMBO J. **7,** 3643–3651.

Levinson, A., Silver, D., and Seed, B. (1984). Minimal size plasmids containing an M13 origin for production of single-strand transducing particles. J. Mol. Appl. Genet. **2,** 507–517.

Metz, J.G., and Miles, D. (1982). Use of a nuclear mutant of maize to identify components of photosystem II. Biochem. Biophys. Acta **681,** 95–102.

Mullet, J.E. (1988). Chloroplast development and gene expression. Annu. Rev. Plant Physiol. Plant Mol. Biol. **39,** 475–502.

Nelson, T., and Langdale, J.A. (1992). Developmental genetics of C4 photosynthesis. Annu. Rev. Plant Physiol. Plant Mol. Biol. **43,** 25–47.

Nelson, T., and Langdale, J.A. (1993). C4 photosynthetic genes and their expression patterns during leaf development. In Control of Plant Gene Expression, D.P.S. Verma, ed (Caldwell, NJ: Telford Press), pp. 259–274.

Nelson, T., Harpster, M.H., Mayfield, S.P., and Taylor, W.C. (1984). Light-regulated gene expression during maize leaf development. J. Cell Biol. **98,** 558–564.

Newton, K.J. (1993). Nonchromosomal stripe mutants of maize. In Plant Mitochondria, A. Brennicke and U. Küch, eds (New York: VCH Publishers), pp. 341–345.

Peterson, P.A. (1960). The pale green mutable system in maize. Genetics **45,** 115–133.

Raghavendra, A.S., Padmasree, K., and Saradadevi, K. (1994). Interdependence of photosynthesis and respiration in plant cells: Interactions between chloroplasts and mitochondria. Plant Sci. **97,** 1–14.

Rao, M.J.K., and Argos, P. (1986). A conformational preference parameter to predict helices in integral membrane proteins. Biochem. Biophys. Acta **869,** 197–214.

Reiter, R.S., Coomber, S.A., Bourett, T.M., Bartley, G.E., and Scolnik, P.A. (1994). Control of leaf and chloroplast development by the Arabidopsis gene *pale cress*. Plant Cell **6,** 1253–1264.

Roussell, D.L., Thompson, D.L., Pallardy, S.G., Miles, D., and Newton, K.J. (1991). Chloroplast structure and function is altered in the NCS2 maize mitochondrial mutant. Plant Physiol. **96,** 232–238.

Schubert, K.R. (1986). Products of biological nitrogen fixation in higher plants: Synthesis, transport, and metabolism. Annu. Rev. Plant Physiol. **37,** 539–574.

Thompson, D., Walbot, V., and Coe, E.H., Jr. (1983). Plastid development in *iojap*- and chloroplast mutator–affected maize plants. Am. J. Bot. **70,** 940–950.

Turner, R.J., Lu, Y., and Switzer, R.L. (1994). Regulation of the *Bacillus subtilis* pyrimidine biosynthetic (*pyr*) gene cluster by an autogenous transcriptional attenuation mechanism. J. Bacteriol. **176,** 3708–3722.

von Heijne, G., Steppuhn, J., and Herrmann, R.G. (1989). Domain structure of mitochondrial and chloroplast targeting peptides. Eur. J. Biochem. **180,** 535–545.

Wetzel, C.M., Jiang, C.-J., Meehan, L.J., Voytas, D.F., and Rodermel, S.R. (1994). Nuclear–organelle interactions: The *immutans* variegation mutant of *Arabidopsis* is plastid-autonomous and impaired in carotenoid biosynthesis. Plant J. **6,** 161–175.